Università di Pisa
Dipartimento di Informatica

Technical Report: TR-01-12

SPECT imaging reconstruction Proposal of an algorithm which exploits the matrix structure

R. Bevilacqua E. Bozzo O. Menchi

June 15, 2001

ADDRESS: Corso Italia 40, 56125 Pisa, Italy. TEL: +39 050 2212700 FAX: +39 050 2212726

SPECT imaging reconstruction
Proposal of an algorithm which exploits the matrix structure

R. Bevilacqua E. Bozzo O. Menchi

June 15, 2001

Abstract

The reconstruction of diagnostic images obtained from SPECT (Single Photon Emission Computed Tomography) requires numerical models which involve structured matrices: Toeplitz and block circulant. In this note an algorithm is proposed, with the aim of exploiting the computational properties enjoyed by these structures.

1 Introduction

The problem considered in this note, a 3D image problem, originates from a diagnostic technique called SPECT (Single Photon Emission Computed Tomography): a patient's body is examined through the emission of γ-rays which are measured by a detector turning around the body. The goal is the reconstruction of some activity map by using a model description of the phenomenon. Let $f(\mathbf{x}, z)$ be the original image, that is the sought for 3D activity distribution at point $(\mathbf{x}, z)$ of the body. The orthogonal reference system is oriented in such a way that the detector rotates around the z-axis. In the $\mathbf{x}$-plane the body of the patient is represented by a disk Ω centered at the origin. The detector plane is perpendicular to the $\mathbf{x}$-plane and the coordinates on it are s and z. Finally ϕ is the projection angle of the detector plane with respect to a fixed position. The rays concentration $g(s, \phi, z)$ is measured at point (s, z) of the detector. Because of the physical structure of the measurement device (the rays pass throught the holes of a collimator) a blur takes place. The blurred image g and the original image f are related by the integral

$$g(s,\phi,z) = \int_{-\infty}^{\infty} \int_{\Omega} \mathcal{F}(s - \mathbf{x}\cdot\boldsymbol{\theta}, z - z', \mathbf{x}\cdot\boldsymbol{\theta}^{\perp})\, f(\mathbf{x}, z')\, d\mathbf{x}\, dz', \tag{1}$$

where $\boldsymbol{\theta} = (\cos\phi, \sin\phi)$, $\boldsymbol{\theta}^{\perp} = (-\sin\phi, \cos\phi)$, the $\cdot$ represents the scalar product between vectors, kernel $\mathcal{F}$ is defined by the function

$$\mathcal{F}(s,z,t) = F_0(s,t)\, F_0(z,t), \quad \text{with} \quad F_0(s,t) = \frac{1}{\sigma(t)\sqrt{2\pi}} \exp\Big[-\frac{s^2}{2\sigma^2(t)}\Big], \tag{2}$$

and

$$\sigma = \sigma_{\min} - \frac{\sigma_{\max} - \sigma_{\min}}{2r}\,(t-r), \text{ with } t \in [-r, r],$$

$r, \sigma_{\min}, \sigma_{\max}$ being given constants.

Model (1) with the kernel (2) is the so-called fully 3D model: it gives accurate results, but its implementation requires too much time. A reduced version, called 2D+1 model, has proved effective from the point of view of both the accuracy and the required computational time. In this model the kernel becomes

$$\mathcal{F}(s, z, t) = F_0(s, t)\; F_0(z, t_{av}), \tag{3}$$

for a suitable fixed value t_{av}. In the following the 2D+1 model will be used. For more detailed information, see [2] and [3].

The problem is then the reconstruction of $f(\mathbf{x}, z)$ from $g(s, \phi, z)$. Because of the deteriorating effects of various physical factors, the measured values of the function $g(s, \phi, z)$ result affected also by a certain amount of noise. The problem is ill-conditioned and a regularized solution is required.

2 Discretization of the problem

Variables ϕ, s and z are discretized at equally spaced nodes:

$\phi_m = m\Delta\phi$, $m = 0, \ldots, M-1$, with $\Delta\phi = 2\pi/M$,

$s_k = s_0 + k\Delta s$, $k = 0, \ldots, K-1$, with $s_K = -s_0$,

$z_l = z_0 + l\Delta z$, $l = 0, \ldots, L-1$, with $z_L = -z_0$.

Typical values for these discretization parameters are $M = 120$ and $K = L = 128$. They are used in this note, together with the the following values for the constants $\sigma_{\min} = 3$, $\sigma_{\max} = 8$, $r = 192$, $\Delta s = \Delta z = 3.2$, $t_{av} = 0$ (all expressed in mm) and the radius of Ω equal to r.

Due to the presence of the collimator filtering the rays, the measure g at each point (s, ϕ, z) of the detector counts all the rays coming throught a hole, thus the discretized value at (s_k, ϕ_m, z_l) is given by

$$g_{kml} = \int_{z_l-\Delta z/2}^{z_l+\Delta z/2} \int_{s_k-\Delta s/2}^{s_k+\Delta s/2} g(s, \phi_m, z)\; ds\; dz.$$

Correspondingly the discretized kernel becomes

$$\mathcal{K}_{kml}(\mathbf{x}, z') = \int_{z_l-\Delta z/2}^{z_l+\Delta z/2} \int_{s_k-\Delta s/2}^{s_k+\Delta s/2} \mathcal{F}(s - \mathbf{x}\cdot\boldsymbol{\theta}_m, z - z', \mathbf{x}\cdot\boldsymbol{\theta}_m^{\perp})\; ds\; dz,$$

where $\boldsymbol{\theta}_m = (\cos\phi_m, \sin\phi_m)$, $\boldsymbol{\theta}_m^{\perp} = (-\sin\phi_m, \cos\phi_m)$. From (3) it follows that

$$\mathcal{K}_{kml}(\mathbf{x}, z') = \mathcal{B}_{km}(\mathbf{x})\mathcal{A}_l(z'),$$

where

$$\mathcal{B}_{km}(\mathbf{x}) = \int_{s_k-\Delta s/2}^{s_k+\Delta s/2} F_0(s - \mathbf{x}\cdot\boldsymbol{\theta}_m, \mathbf{x}\cdot\boldsymbol{\theta}_m^{\perp})\ ds,$$

$$\mathcal{A}_l(z') = \int_{z_l-\Delta z/2}^{z_l+\Delta z/2} F_0(z - z', t_{av})\ dz,$$

and from equation (1) we get

$$g_{kml} = \int_{-\infty}^{\infty}\int_{\Omega} \mathcal{B}_{km}(\mathbf{x})\mathcal{A}_l(z')\ f(\mathbf{x}, z')\ d\mathbf{x}\ dz'. \tag{4}$$

Equation (4) defines a linear operator R mapping $L^2(\Omega)$ on $\mathbf{R}^q$, with $q = KML$, such that

$$\begin{aligned} R\ :\ f(\mathbf{x}, z')\ &\rightarrow\ \mathbf{g}, \quad \text{where} \\ \mathbf{g} = \{g_{kml}\},\ k &= 0, \ldots, K-1\ ,\ m = 0, \ldots, M-1\ ,\ l = 0, \ldots, L-1. \end{aligned}$$

Since the equation $Rf = \mathbf{g}$ is underdetermined, we look for the generalized solution

$$f^* = R^*\mathbf{h}, \quad \text{where} \quad RR^*\mathbf{h} = \mathbf{g},$$

and R^* is the adjoint operator of R. The operator RR^* maps $\mathbf{R}^q$ on itself, then $\mathbf{h}$ is the solution of a linear system of dimension q which we write as

$$H\mathbf{h} = \mathbf{g}. \tag{5}$$

With the values chosen for the discretization the size of system (5) is $q = 983040$. Due to the large dimensions, any attempt to solve system (5) without exploiting the structure of H would be fruitless. Fortunately the separability of the kernel in (4) and the translational and rotational invariance of the SPECT system reflect into a strong structure of H.

3 Structure of the matrix H

The entries of the matrix H are given by scalar products of the kernel $\mathcal{B}_{km}(\mathbf{x})\mathcal{A}_l(z')$ of (4), that is

$$h_{kml,k'm'l'} = \int_{\Omega} \mathcal{B}_{km}(\mathbf{x})\mathcal{B}_{k'm'}(\mathbf{x})\ d\mathbf{x}\ \int_{-\infty}^{\infty} \mathcal{A}_l(\zeta)\mathcal{A}_{l'}(\zeta)\ d\zeta.$$

Hence from the separability of the kernel it follows that the matrix H can be written as the tensor product $H = A \otimes B$, where A and B are the Gram matrices of the functions $\mathcal{A}_l(z)$ and $\mathcal{B}_{km}(\mathbf{x})$ respectively, that is the elements of A and B are given by the scalar products

$$a_{l,l'} = \int_{-\infty}^{\infty} \mathcal{A}_l(\zeta)\mathcal{A}_{l'}(\zeta)\ d\zeta, \quad b_{km,k'm'} = \int_{\Omega} \mathcal{B}_{km}(\mathbf{x})\mathcal{B}_{k'm'}(\mathbf{x})\ d\mathbf{x}. \tag{6}$$

The dimensions of the matrices A and B are L and $P = KM$ respectively. System (5) can then be written as $(A \otimes B)\mathbf{h}$. A property of the tensor product allows the decoupling of this system into the two systems

$$(A \otimes I_P)\,\mathbf{y} = \mathbf{g} \tag{7}$$

$$(I_L \otimes B)\,\mathbf{h} = \mathbf{y}, \tag{8}$$

where I_q and I_L are the identity matrices of size P and L resp. Equation (7) corresponds to a sequence of P systems of size L and equation (8) corresponds to a sequence of L systems of size P. With the values chosen for the discretization it is $L = 64$ and $P = 15360$. Systems (8) are still too large to be treated.

But matrices A and B enjoy additional structures which are inherited from invariance properties of the SPECT system. Let us examine first matrix A. Being a Gram matrix, A is symmetric and semidefinite positive. Moreover, from (6) we have

$$a_{l,l'} = \int_{z_l-\Delta z/2}^{z_l+\Delta z/2} \int_{z'_l-\Delta z/2}^{z'_l+\Delta z/2} \alpha(z,z')\ dz\ dz',$$

where

$$\alpha(z,z') = \int_{-\infty}^{\infty} F_0(z-\zeta,t_{av})F_0(z'-\zeta,t_{av})\ d\zeta.$$

From (2), remembering that

$$\int_{-\infty}^{\infty} \exp\Big[-\frac{(z-\zeta)^2+(z'-\zeta)^2}{c}\Big]\ d\zeta = \sqrt{\frac{c\pi}{2}}\ \exp\Big[-\frac{(z-z')^2}{2c}\Big],$$

we get

$$a_{l,l'} = \frac{1}{\sigma(t_{av})2\sqrt{\pi}} \int_{z_l-\Delta z/2}^{z_l+\Delta z/2} \int_{z_{l'}-\Delta z/2}^{z_{l'}+\Delta z/2} \exp\Big[-\frac{(z-z')^2}{4\sigma^2(t_{av})}\Big]\ dz\ dz',$$

and by a suitable change of variable

$$a_{l,l'} = \frac{1}{\sigma(t_{av})2\sqrt{\pi}} \int_0^{\Delta z} \int_0^{\Delta z} \exp\Big[-\frac{(z-z'+(l-l')\Delta z)^2}{4\sigma^2(t_{av})}\Big]\ dz\ dz'.$$

Thus A is the Toeplitz matrix

$$A = \begin{bmatrix} a_0 & a_1 & a_2 & \dots & a_{L-1} \\ a_1 & \ddots & \ddots & \ddots & \\ a_2 & \ddots & \ddots & \ddots & \\ \vdots & & \ddots & \ddots & a_1 \\ a_{L-1} & & & a_1 & a_0 \end{bmatrix}, \quad \text{where} \quad a_i = a_{i,0}.$$

Note that A depends only on Δz and $\sigma(t_{av})$.

Matrix B can be seen as a $M \times M$ block matrix, with blocks $B_{m,m'}$, for $m,\ m' = 0, \ldots, M-1$. The (k,k')-entry of $K \times K$ block $B_{m,m'}$ is

$$b_{km,k'm'} = \int_{s_k-\Delta s/2}^{s_k+\Delta s/2} \int_{s_{k'}-\Delta s/2}^{s_{k'}+\Delta s/2} \beta_{m,m'}(s,s')\ ds\ ds' \tag{9}$$

where

$$\beta_{m,m'}(s,s') = \int_\Omega F_0(s - \mathbf{x} \cdot \boldsymbol{\theta}_m, \mathbf{x} \cdot \boldsymbol{\theta}_m^\perp)\ F_0(s' - \mathbf{x} \cdot \boldsymbol{\theta}_{m'}, \mathbf{x} \cdot \boldsymbol{\theta}_{m'}^\perp)\ d\mathbf{x}. \tag{10}$$

Being a Gram matrix, B is symmetric and semidefinite positive. Hence

$$B_{m,m'} = B_{m',m}^T, \quad \text{for} \quad m,\ m' = 0, \ldots, M-1. \tag{11}$$

Moreover, let

$$U = \begin{bmatrix} \cos \Delta\theta & \sin \Delta\theta \\ -\sin \Delta\theta & \cos \Delta\theta \end{bmatrix}$$

be the unitary rotational operator. It verifies $\mathbf{x} \cdot \boldsymbol{\theta}_{m+1} = (U\mathbf{x}) \cdot \boldsymbol{\theta}_m$ and $\mathbf{x} \cdot \boldsymbol{\theta}_{m+1}^\perp = (U\mathbf{x}) \cdot \boldsymbol{\theta}_m^\perp$. Then for any s and s'

$$\beta_{m+1,m'+1}(s,s') = \int_\Omega F_0(s - (U\mathbf{x}) \cdot \boldsymbol{\theta}_m, (U\mathbf{x}) \cdot \boldsymbol{\theta}_m^\perp)\ F_0(s' - (U\mathbf{x}) \cdot \boldsymbol{\theta}_m, (U\mathbf{x}) \cdot \boldsymbol{\theta}_m^\perp)\ d\mathbf{x}.$$

Performing the change of variable $\mathbf{y} = U\mathbf{x}$ and taking into account that this change maps the disk Ω on itself, it turns out that $\beta_{m+1,m'+1}(s,s') = \beta_{m,m'}(s,s')$. Moreover, since $\boldsymbol{\theta}_M = \boldsymbol{\theta}_0$, it turns out that $\beta_{1,0}(s,s') = \beta_{0,M-1}(s,s')$. These relations say that B is the circulant block matrix

$$B = \begin{bmatrix} B_0 & B_1 & B_2 & \ldots & B_{M-1} \\ B_{M-1} & B_0 & B_1 & \ddots & \\ \vdots & \ddots & \ddots & \ddots & \\ \vdots & & \ddots & \ddots & B_1 \\ B_1 & B_2 & \ldots & B_{M-1} & B_0 \end{bmatrix}, \quad \text{where} \quad B_m = B_{0,m}.$$

From (11) it follows that blocks B_0 and $B_{M/2}$ are symmetric and

$$B_{M-m} = B_m^T, \quad \text{for} \quad m = 1, \ldots, M/2 - 1. \tag{12}$$

A further structure can be recognized comparing the (k,k')-element of block B_m with the $(K-k-1, K-k'-1)$-element of block B_{M-m}, that is the entries $b_{k0,k'm}$ and $b_{K-k-1,0,K-k'-1,M-m}$. We have

$$\beta_{0,m}(s,s') = \int_\Omega F_0(s - \mathbf{x} \cdot \boldsymbol{\theta}_0, \mathbf{x} \cdot \boldsymbol{\theta}_0^\perp)\ F_0(s' - \mathbf{x} \cdot \boldsymbol{\theta}_m, \mathbf{x} \cdot \boldsymbol{\theta}_m^\perp)\ d\mathbf{x}$$

and

$$\beta_{0,M-m}(-s,-s') = \int_\Omega F_0(-s - \mathbf{x} \cdot \boldsymbol{\theta}_0, \mathbf{x} \cdot \boldsymbol{\theta}_0^\perp)\ F_0(-s' - \mathbf{x} \cdot \boldsymbol{\theta}_{M-m}, \mathbf{x} \cdot \boldsymbol{\theta}_{M-m}^\perp)\ d\mathbf{x}.$$

Let $\mathbf{x} = (x_1, x_2)$. Then

$$\begin{aligned}
&\mathbf{x}\cdot\boldsymbol{\theta}_0 = x_1,\ \mathbf{x}\cdot\boldsymbol{\theta}_0^\perp = x_2,\\
&\mathbf{x}\cdot\boldsymbol{\theta}_m = x_1\cos\phi_m + x_2\sin\phi_m,\ \mathbf{x}\cdot\boldsymbol{\theta}_m^\perp = -x_1\sin\phi_m + x_2\cos\phi_m,\\
&\mathbf{x}\cdot\boldsymbol{\theta}_{M-m} = x_1\cos\phi_m - x_2\sin\phi_m,\ \mathbf{x}\cdot\boldsymbol{\theta}_{M-m}^\perp = x_1\sin\phi_m + x_2\cos\phi_m.
\end{aligned}$$

By making the change of variable $y_1 = -x_1$ and taking into account that the disk Ω is symmetric around the x_2-axis, we get $\beta_{0,m}(s,s') = \beta_{0,M-m}(-s,-s')$. Since $s_{K-k-1} = -s_k$, this means that the (k,k')-element of block B_m is equal to the $(K-k-1, K-k'-1)$-element of block B_{M-m}, that is

$$B_{M-m} = JB_mJ, \quad \text{where} \quad J = \begin{bmatrix} & & & 1\\ & & 1 & \\ & \cdot^{\cdot^{\cdot}} & & \\ 1 & & & \end{bmatrix}. \tag{13}$$

Hence $B_m^T = JB_mJ$, that is B_m is persymmetric. Then

$$(B_{M-m})_{ij} = (B_m)_{K-i,K-j} = (B_m)_{ji}, \quad \text{for} \quad i,\ j = 0,\ldots,K. \tag{14}$$

To indicate properties (12) and (14) we use the notation $B_{M-m} = B_m^\times$. Blocks B_0 and $B_{M/2}$ satisfy $B_0 = B_0^\times$ and $B_{M/2} = B_{M/2}^\times$, thus they are centersymmetric. In conclusion the first block line of the matrix B has the form

$$\begin{bmatrix} B_0 & B_1 & \ldots & B_{M/2-1} & B_{M/2} & B_{M/2-1}^\times & \ldots B_1^\times \end{bmatrix}.$$

In the following description of the algorithms for solving systems (7) and (8) we make use of two operators which estract subvectors from a vector $\mathbf{v}$ of length $m\,n$:

(a) the operator $\chi\ :\ \{0,\ldots,n-1\}\times\mathbf{R}^{m\,n} \to \mathbf{R}^m$ defined by

$$\chi_n(j,\mathbf{v}) = \mathbf{v}^{(j)}, \quad j = 0,\ldots,n-1, \quad \text{where} \quad v_i^{(j)} = v_{i\,n+j}, \quad i = 0,\ldots,m-1.$$

(b) the operator $\psi\ :\ \{0,\ldots,m-1\}\times\mathbf{R}^{m\,n} \to \mathbf{R}^n$ defined by

$$\psi_n(j,\mathbf{v}) = \mathbf{v}^{(j)}, \quad j = 0,\ldots,m-1, \quad \text{where} \quad v_i^{(j)} = v_{j\,n+i}, \quad i = 0,\ldots,n-1.$$

4 Solving system (7)

Vector $\mathbf{g}$ is assumed to be stored by column in such a way that $g_{kml} = g_{(lM+m)K+k}$, for $k = 0,\ldots,K-1$, $m = 0,\ldots,M-1$, $l = 0,\ldots,L-1$. The P systems corresponding to (7) are then

$$A\,\chi_P(p,\mathbf{y}) = \chi_P(p,\mathbf{g}), \quad \text{for} \quad p = 0,\ldots,P-1.$$

By setting $\mathbf{u} = \chi_P(p, \mathbf{y})$ and $\mathbf{w} = \chi_P(p, \mathbf{g})$, we concentrate on solving the p-th system, written as

$$A\,\mathbf{u} = \mathbf{w}. \tag{15}$$

This system has a symmetric Toeplitz matrix, whose first line is

$$\Big[a_0, a_1, \ldots, a_{L-1}\Big],$$

where

$$a_i = \frac{1}{2\sigma(t_{av})\sqrt{\pi}} \int_0^{\Delta z} \int_0^{\Delta z} \exp\Big[-\frac{(z - z' + i\Delta z)^2}{4\sigma^2(t_{av})}\Big]\, dz\, dz'.$$

Since we are interested into computing a regularized solution, we can can use one of the regularizing methods described in the literature [1]. Here we examine the following ones:

(a) (Tikhonov regularization) choose a suitable regularization parameter μ, tuned with the noise which affects the blurred image, and solve the system

$$(A + \mu I_L)\mathbf{u} = \mathbf{w} \tag{16}$$

by using a direct method based on a factorization of matrix A. Of course the factorization should be computed only once and used for all the P systems (16).

(b) solve system (15) by using an iterative method which enjoys the regularizing property. The iteration should be stopped before the noise starts to corrupt the computed solution. Since A is symmetric and definite positive the CG method is chosen.

(c) solve system (15) by using a truncated SVD.

In our case, where A is a small size matrix, any strategy is applicable. Numerical experiments (see section 7) have been conducted on system (15) in order to

(a) determine a safe chop level for the coefficients of the system,

(b) study the regularizing effectiveness of technique (16) and find the best value μ,

(c) examine if a preconditioner is required by the CG method, according to noise.

(d) study the best threshold value for the SVD.

(e) compare the results from the point of view of the cost and of the regularizing effectiveness.

5 Solving system (8)

The L systems corresponding to (8) are

$$B\,\psi_P(l,\mathbf{h}) = \psi_P(l,\mathbf{y}), \quad \text{for} \quad l = 0,\ldots,L-1.$$

By setting $\mathbf{u} = \psi_P(l,\mathbf{h})$ and $\mathbf{w} = \psi_P(l,\mathbf{y})$, we concentrate on solving the l-th system, written as

$$B\,\mathbf{u} = \mathbf{w}. \tag{17}$$

Due to the circulant structure of the matrix B a direct method is suggested for solving (17), at least at the outer level. The first block line of the matrix B is

$$\begin{bmatrix} B_0 & B_1 & \ldots & B_{M/2-1} & B_{M/2} & B^{\times}_{M/2-1} & \ldots B^{\times}_1 \end{bmatrix}.$$

It is well known that the $P \times P$ matrix B can be block diagonalized by means of the matrix $F_M \otimes I_K$, where F_M is the $M \times M$ Fourier matrix whose elements are $f_{i,j} = \omega^{ij}/\sqrt{M}$, for $i,\ j = 0,\ldots,M-1$, with $\omega = \exp(\mathbf{i}\,2\pi/M)$, that is

$$B = (F_M \otimes I_K)D(F_M \otimes I_K)^H,$$

where

$$D = \sum_{t=0}^{M-1}(\Omega^t \otimes B_t), \qquad \Omega = \begin{bmatrix} 1 & & & \\ & \omega & & \\ & & \ddots & \\ & & & \omega^{M-1} \end{bmatrix}. \tag{18}$$

D is the block diagonal matrix

$$D = \begin{bmatrix} D_0 & & & \\ & D_1 & & \\ & & \ddots & \\ & & & D_{M-1} \end{bmatrix}, \quad \text{with} \quad D_\tau = \sum_{t=0}^{M-1}\omega^{\tau t}B_t. \tag{19}$$

The best way to compute the $K \times K$ blocks D_τ is to make use of a fast Fourier transform. In fact, for each pair of indices i and j from (19) we have

$$(D_\tau)_{ij} = \sum_{t=0}^{M-1}\omega^{\tau t}(B_t)_{ij},$$

and by considering the vectors

$$\mathbf{b} = \Big(\ (B_0)_{ij}, (B_1)_{ij}, \ldots, (B_{M-1})_{ij}\ \Big), \qquad \mathbf{d} = DFT(\mathbf{b})\,\sqrt{M},$$

we have $(D_\tau)_{i,j} = d_\tau$. From (14) it follows that

$$\mathbf{b} = \Big(\ (B_0)_{ij}, (B_1)_{ij}, \ldots, (B_{M/2-1})_{ij}, (B_{M/2})_{ij}, (B_{M/2-1})_{ji}, \ldots, (B_1)_{ji}\ \Big) \tag{20}$$

We now examine the structure of the blocks D_τ. Since M is an even integer and for each $i,\ j$ the elements of $\mathbf{b}$ are real numbers, the elements of the vector $\mathbf{d}$ satisfy:

(a) d_0 and $d_{M/2}$ are real numbers,

(b) $d_\tau = \overline{d}_{M-\tau}$ for $\tau = 1, \dots, M/2 - 1$.

It follows that D_0 and $D_{M/2}$ are real and $D_\tau = \overline{D}_{M-\tau}$ for $\tau = 1, \dots, M/2 - 1$. Moreover from (19) we have

$$D_\tau = B_0 + (-1)^\tau \; B_{M/2} + \sum_{t=1}^{M/2-1} \left(\omega^{\tau t} B_t + \overline{\omega}^{\tau t} B_t^\times \right).$$

Since B_0 and $B_{M/2}$ are symmetric and centersymmetric, it follows that

$$D_\tau^H = B_0 + (-1)^\tau \; B_{M/2} + \sum_{t=1}^{M/2-1} \left(\overline{\omega}^{\tau t} B_t^T + \omega^{\tau t} B_t \right) = D_\tau,$$

$$J\overline{D}_\tau J = B_0 + (-1)^\tau \; B_{M/2} + \sum_{t=1}^{M/2-1} \left(\overline{\omega}^{\tau t} B_t^\times + \omega^{\tau t} B_t \right) = D_\tau,$$

that is D_τ is hermitian and centerhermitian. It follows that only the elements $(D_\tau)_{ij}$, with $i = 0, \dots, K/2$ and $j = i, \dots, K-i-1$ must be effectively computed, since all the other elements of D_τ can be constructed from them.

From 18) it follows that

$$D \; (F_M^H \otimes I_K) \; \mathbf{u} = (F_M^H \otimes I_K) \; \mathbf{w}. \tag{21}$$

Equation (21) corresponds to a sequence of M systems of size K. The vector $\mathbf{v} = (F_M^H \otimes I_K) \; \mathbf{w}$ can be computed in the following way: for $k = 0, \dots, K-1$

(a) consider the subvectors $\mathbf{w}^{(k)} = \chi_K(k, \mathbf{w})$ of size M,

(b) compute $\mathbf{f}^{(k)} = F_M^H \mathbf{w}^{(k)}$ by using the IDFT.

Then $\mathbf{v}$ is the vector such that $\chi_K(k, \mathbf{v}) = \mathbf{f}^{(k)}$. The elements of the vectors $\mathbf{f}^{(k)}$ satisfy $f_\tau^{(k)} = \overline{f}_{M-\tau}^{(k)}$ for $\tau = 1, \dots, M/2 - 1$. Moreover $f_0^{(k)}$ and $f_{M/2}^{(k)}$ are real.

System (21) becomes

$$D \; \mathbf{t} = \mathbf{v}, \tag{22}$$

where $\mathbf{u} = (F_M \otimes I_K)\mathbf{t}$. Once $\mathbf{t}$ has been computed by solving (22), $\mathbf{u}$ is retrieved through the DFT. By rewriting (22) in terms of blocks we have

$$D_\tau \; \psi_K(\tau, \mathbf{t}) = \psi_K(\tau, \mathbf{v}), \quad \text{for} \quad \tau = 0, \dots, M-1. \tag{23}$$

It is easy to verify that $\psi_K(\tau, \mathbf{v}) = \overline{\psi}_K(M-\tau, \mathbf{v})$ for $\tau = 1, \dots, M/2 - 1$ and that $\psi_K(0, \mathbf{v})$ and $\psi_K(M/2, \mathbf{v})$ are real. Hence of all the systems (23) only those corresponding to indices $\tau = 0, \dots, M/2$ must be solved, since a system with index $\tau > M/2$ has the coefficient matrix and the second-hand vector which are the conjugate of the coefficient matrix and the second-hand vector of the system with index $M - \tau$.

By setting $\mathbf{u} = \psi_K(\tau, \mathbf{t})$ and $\mathbf{z} = \psi_K(\tau, \mathbf{v})$, we concentrate on solving the τ-th system for $\tau = 0, \dots, M/2$, written as

$$D_\tau\, \mathbf{u} = \mathbf{z}, \tag{24}$$

where

(a) D_0 is real, symmetric and centersymmetric, the corresponding $\mathbf{z}$ is real,

(b) D_τ is complex, hermitian and centerhermitian for $\tau = 0, \dots, M/2-1$,

(c) $D_{M/2}$ is real, symmetric and centersymmetric, the corresponding $\mathbf{z}$ is real.

6 Solving systems (24)

Each system (24) has size K and, with the exception of the first and last system, is complex. In general the solution of a $K \times K$ complex system requires solving a $2K \times 2K$ real system. But in the present case the complexity can be reduced, because of the structure of matrices D_τ. In this section we denote by I the identity matrix of size $K/2$ and by J the reverse permutation matrix of size $K/2$.

Since D_τ is centerhermitian, system (24) can be written in the following way (drop for the moment the index τ)

$$\begin{bmatrix} C_1 & C_2\, J \\ J\, \overline{C}_2 & J\, \overline{C}_1\, J \end{bmatrix} \begin{bmatrix} \mathbf{u}_1 \\ \mathbf{u}_2 \end{bmatrix} = \begin{bmatrix} \mathbf{z}_1 \\ \mathbf{z}_2 \end{bmatrix}, \tag{27}$$

where C_1 and C_2 are $K/2 \times K/2$ complex blocks and $\mathbf{z}_1$ and $\mathbf{z}_2$ are $K/2$ complex vectors. Moreover, since D_τ is hermitian, C_1 is hermitian and C_2 is symmetric. The upper triangular parts of C_1 and C_2 are given by

$$\begin{gathered} (C_1)_{ij} = (D_\tau)_{ij}, \quad (C_2)_{ij} = (D_\tau)_{i,M-j-1} \\ \text{for} \quad i = 0, \dots, M/2-1,\ j = i, \dots, M/2-1. \end{gathered} \tag{28}$$

Let us examine first the real case. If $\tau = 0$ or $\tau = M/2$, the matrix of the system is

$$D_\tau = \begin{bmatrix} C_1 & C_2\, J \\ J\, C_2 & J\, C_1\, J \end{bmatrix},$$

with C_1 and C_2 symmetric, and can be block diagonalized by the matrix

$$\Pi = \begin{bmatrix} I & J \\ I & -J \end{bmatrix}.$$

In fact

$$D_\tau = \frac{1}{2}\, \Pi^T \begin{bmatrix} C_1 + C_2 & O \\ O & C_1 - C_2 \end{bmatrix} \Pi.$$

In this case system (27) reduces to

$$\begin{bmatrix} C_1+C_2 & O \\ O & C_1-C_2 \end{bmatrix} \begin{bmatrix} \mathbf{u}_1+J\mathbf{u}_2 \\ \mathbf{u}_1-J\mathbf{u}_2 \end{bmatrix} = \begin{bmatrix} \mathbf{z}_1+J\mathbf{z}_2 \\ \mathbf{z}_1-J\mathbf{z}_2 \end{bmatrix}.$$

Thus $\mathbf{u}_1$ and $\mathbf{u}_2$ can be retrieved by solving two $K/2 \times K/2$ real symmetric systems.

If $0 < \tau < M/2$, we apply to system (27) the matrix

$$\Pi = \begin{bmatrix} I & J \\ \mathbf{i}I & -\mathbf{i}J \end{bmatrix}.$$

System (27) reduces to

$$\begin{bmatrix} C_{11} & C_{12} \\ C_{21} & C_{22} \end{bmatrix} \begin{bmatrix} \mathbf{u}_{11} & \mathbf{u}_{12} \\ \mathbf{u}_{21} & \mathbf{u}_{22} \end{bmatrix} = \begin{bmatrix} \mathbf{z}_{11} & \mathbf{z}_{12} \\ \mathbf{z}_{21} & \mathbf{z}_{22} \end{bmatrix}, \tag{29}$$

where

$$\begin{gathered}
C_{11} = C_1^{(re)} + C_2^{(re)},\ C_{12} = C_1^{(im)} - C_2^{(im)}, \\
C_{21} = -C_1^{(im)} - C_2^{(im)},\ C_{22} = C_1^{(re)} - C_2^{(re)}, \\
\mathbf{u}_{11} = \mathbf{u}_1^{(re)} + J\mathbf{u}_2^{(re)},\ \mathbf{u}_{12} = \mathbf{u}_1^{(im)} + J\mathbf{u}_2^{(im)}, \\
\mathbf{u}_{21} = -\mathbf{u}_1^{(im)} + J\mathbf{u}_2^{(im)},\ \mathbf{u}_{22} = \mathbf{u}_1^{(re)} - J\mathbf{u}_2^{(re)}, \\
\mathbf{z}_{11} = \mathbf{z}_1^{(re)} + J\mathbf{z}_2^{(re)},\ \mathbf{z}_{12} = \mathbf{z}_1^{(im)} + J\mathbf{z}_2^{(im)}, \\
\mathbf{z}_{21} = -\mathbf{z}_1^{(im)} + J\mathbf{z}_2^{(im)},\ \mathbf{z}_{22} = \mathbf{z}_1^{(re)} - J\mathbf{z}_2^{(re)}.
\end{gathered}$$

Thus $\mathbf{u}_1$ and $\mathbf{u}_2$ can be retrieved by solving a $K \times K$ real system with matrix

$$E_\tau = \Pi D_\tau \Pi^H = \begin{bmatrix} C_{11} & C_{12} \\ C_{21} & C_{22} \end{bmatrix} \tag{30}$$

and two different real right-hand sides. Since $C_1^{(re)}$, $C_2^{(re)}$ and $C_2^{(im)}$ are symmetric and $C_1^{(im)}$ is antisymmetric, then C_{11} and C_{22} are symmetric and $C_{12} = C_{21}^T$. Hence E_τ is symmetric and semidefinite positive. There are L systems like (29) to be solved with the same matrix E_τ and different right-hand sides.

7 Numerical experiments on system (7)

Matrix A is very close to the Gaussian Toeplitz matrix G whose first row elements are

$$t_i = \gamma\ \exp(-\delta\, i^2), \quad \text{where} \quad \gamma = \frac{\Delta z^2}{2\sigma(t_{av})\sqrt{\pi}}, \quad \delta = \frac{\Delta z^2}{4\sigma^2(t_{av})},$$

which is notoriously ill-conditioned when δ is small. In our case it is $\delta \approx 0.074$ and the condition number of A turns out to be greater than 10^7.

As it is customary, we scale the coefficients of A by dividing by the quantity $scal = a_0 + 2\sum_{i=1}^{L} a_i$. Now the values of a_i range from 0.212366 for $i = 0$ down to $2.53659\ 10^{-15}$ for $i = 15$. For $i > 15$, a_i can be considered zero. In this way A becomes a band matrix with bandwith $b = 15$.

7.1 - Bandwidth determination. The first numerical experiment has the aim to find if the bandwidth can be safely reduced. A set S of vectors $\mathbf{s}$ of size L has been randomly generated. For $i = 1, \ldots, 14$ the matrix A_t with bandwith i has been obtained by cutting the coefficient of A with index greater than i. The two solutions

$$A\,\mathbf{x} = \mathbf{s}, \quad A_t\,\mathbf{y} = \mathbf{s}$$

have been computed with their relative norm 2 error $\|\mathbf{x}-\mathbf{y}\|_2/\|\mathbf{x}\|_2$. The average error E over the set S is shown in Table 1, together with the value of the greatest cut coefficient. The errors E for $i < 9$ are greater than 0.5 and are not shown.

i	a_{i+1}	E
9	$1.44\ 10^{-7}$	$2.44\ 10^{-1}$
10	$7.21\ 10^{-9}$	$1.48\ 10^{-2}$
11	$2.71\ 10^{-10}$	$4.85\ 10^{-4}$
12	$7.63\ 10^{-12}$	$1.57\ 10^{-5}$
13	$1.61\ 10^{-13}$	$3.37\ 10^{-7}$
14	$2.54\ 10^{-15}$	$5.31\ 10^{-9}$

Table 1 - Norm 2 errors of the solution of the cut matrix A.

Such great errors are easily explained by the high condition number of A. It is evident that the bandwidth cannot be reduced under 10. Since the cost of the multiplication of a band matrix for a vector is a linear function of the bandwidth, we suggest to keep more coefficients. For $\omega = 12$ the already scaled values are

$$\begin{gathered} a_0 = 0.212366,\ a_1 = 0.18432,\ a_2 = 0.120506,\ a_3 = 0.0593362,\ a_4 = 0.0219982, \\ a_5 = 0.00613834,\ a_6 = 0.00128858,\ a_7 = 0.000203396,\ a_8 = 0.0000241263, \\ a_9 = 2.14927\ 10^{-6},\ a_{10} = 1.43703\ 10^{-7},\ a_{11} = 7.20667\ 10^{-9},\ a_{12} = 2.70905\ 10^{-10}. \end{gathered} \tag{31}$$

The corresponding scaling factor is $scal = 2.12132$.

The following experiments have been carried out by choosing a reference solution $\mathbf{x}$ and computing $A\mathbf{x}$ of components so defined: $x_i = 100$ if $L/8 \le i \le 3L/8$ or $5L/8 \le i \le 7L/8$, and computing $A\mathbf{x}$ with the original matrix A. Then the cut version with the bandwidth $\omega = 12$ has been used for the reconstruction tests. The experiments have been made on a noisy blurred image, obtained by multiplying the solution $\mathbf{x}$ by A and adding a vector $\boldsymbol{\eta}$ of randomly generated entries with Poisson distribution and mean 0.5. The entries of $\boldsymbol{\eta}$ are scaled in

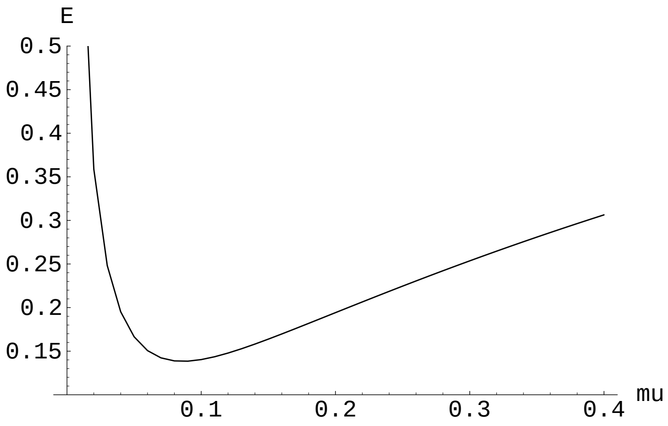

Figure 1: E versus μ for the noise level 10^{-2}.

such a way that $\|\boldsymbol{\eta}\|_2/\|A\mathbf{x}\|_2 = 10^{-k}$, for increasing values of k. Typical values for k in practice are around 2, thus it seems useless to consider values of k greater than 3. The vector $\mathbf{w}$ so obtained is the right-hand side of system (15) and the norm 2 error E of the solution computed with respect to $\mathbf{x}$ is considered.

Since the solution of (7) becomes the right-hand side of the system (8), it should be computed with the least possible error E, even if this requires more operations (but not too many, due to the large number of systems (15) to be solved).

7.2 - Tikhonov regularization. Different values of regularization parameter μ have been chosen for system (16), which has been solved through the Choleski factorization. Fig. 1 shows the behaviour of E as a function of μ for case $k = 2$. As expected, when μ is increased until an optimal value μ_{opt}, the values of E decrease until value E_{opt} is obtained, then increase. Values for μ greater than μ_{opt} would be safer than smaller values. Table 2 shows μ_{opt} and E_{opt} for different k.

k	μ_{opt}	E_{opt}
1	$3.1\ 10^{-1}$	$3.09\ 10^{-1}$
2	$8.\ 10^{-2}$	$1.34\ 10^{-1}$
3	$2.\ 10^{-2}$	$7.78\ 10^{-2}$

Table 2 - Norm 2 errors of the solution of the reconstructed image computed by solving (16).

The computational cost is $\omega^2 L$ for the preprocessing phase and $2\omega L$ for the substitution phase.

7.3 - Non-preconditioned CG method. The CG method has been applied to the same right-hand side used for the Tikhonov regularization experiment, starting with the zero vector. Table 3 shows the optimal values of E obtained for different noise levels together with the required iteration numbers.

k	it_{opt}	E_{opt}
1	1	$4.31\ 10^{-2}$
2	3	$2.32\ 10^{-2}$
3	8	$1.7\ 10^{-2}$

Table 3 - Norm 2 errors of the solution of the reconstructed image computed by CG.

For $k = 2, 3$ the value of E is less than $2.5\ 10^{-2}$ already after two iterations. This suggests to perform always two iterations of the CG method, regardless of the noise level.

Since the cost of each CG iteration is about $2\omega L$, the cost for two iterations is the double than with the Tikhonov regularization, but the regularization effectiveness is much better for the CG. Anyway no preconditioner seems to be required, due to the small number of iterations.

7.4 - Truncated SVD. Also this method has been applied to the same right-hand side used for the Tikhonov regularization experiment. Singular values and vectors of A have been computed: 67 singular values out of 128 are over 10^{-2}. Table 4 shows for the various noise levels the best threshold ϵ_{opt} to be used, the number i_{opt} of singular values greater than ϵ_{opt} and the corresponding E_{opt} obtained.

k	ϵ_{opt}	i_{opt}	E_{opt}
1	$2.5\ 10^{-1}$	36	$1.21\ 10^{-1}$
2	$4.5\ 10^{-2}$	56	$8.73\ 10^{-2}$
3	$1.\ 10^{-2}$	67	$6.74\ 10^{-2}$

Table 4 - Norm 2 errors of the solution of the reconstructed image computed by the truncated SVD.

Since the cost for each term of the SVD is about $2L$, the totla cost for 36, 56 or 67 terms is much higher than the cost of the two previous methods. In order to compare the truncated SVD with the other methods on a same cost basis, the threshold $\epsilon = 0.85$ is selected. In this way only 12 terms are added, with the same cost of the Tikhonov method. The norm 2 error E of the computed solution is about $2.12\ 10^{-1}$, regardless of the noise level.

7.5 - Conclusion on the test results for system (7). In the choice of the method to use for solving system (15) one should take into account that

(a) the truncated SVD has a much higher preprocessing cost of the other method (CG method has no preprocessing cost).

(b) Tikhonov method requires the memorization of the Choleski factor and the truncated SVD needs the singular vectors, while the CG method requires only the $\omega + 1$ values a_i.

(c) CG regularizing effectiveness appears superior.

All considered, we suggest to use the CG method, even if it costs the double than the Tikhonov method.

8 Numerical experiments on system (8)

For $k = 0, \ldots, K/2$ and $k' = k, \ldots, K - k - 1$ the entries of the vector $\mathbf{b}$ of (20) are given by (9): its m-th element is

$$b_m = \int_{s_k - \Delta s/2}^{s_k + \Delta s/2} \int_{s_{k'} - \Delta s/2}^{s_{k'} + \Delta s/2} \beta_{0,m}(s, s')\, ds\, ds', \quad \text{for} \quad m = 0, \ldots, M/2, \tag{32}$$

and

$$b_{M-m} = \int_{s_k - \Delta s/2}^{s_k + \Delta s/2} \int_{s_{k'} - \Delta s/2}^{s_{k'} + \Delta s/2} \beta_{0,m}(s, s')\, ds\, ds', \quad \text{for} \quad m = 1, \ldots, M/2 - 1. \tag{33}$$

For the experiments the integrals have been computed by using a high precision adaptive integration method. Then the blocks D_τ for $\tau = 0, \ldots, M/2$ have been computed by using a fast DFT routine.

8.1 - Conditioning of the blocks D_τ. The first numerical experiment has the aim to find how the condition numbers of the blocks D_τ depend on the precision of the integration process. It turns out that the higher the precision, the higher the condition numbers. This property follows from the fact that the original continuous problem is ill-conditioned. Hence the ill-conditioning of the discrete problem is higher when the approximation is more refined. But the number of the singular values of the blocks D_τ that are not clustered around zero is independent from the precision of the integration process. Moreover the values of the highest singular values and of the corresponding singular vectors are only marginally affected. For this reason a high precision in computing the integrals is not effectively required. A 10^{-6} precision turns out to be a good compromise between computational costs and acceptable image reconstruction.

Examining in detail the conditioning of each block D_τ, it turns out that the conditioning tends to decrease when the index τ increases from 0 to $M/2$, that is the first blocks have the highest conditioning. A consequence of this situation is that the first blocks allow a better separation of the signal subspace from the noise subspace.

8.2 - Noise levels of the right-hand sides. A reference solution $\mathbf{u}$ for the systems (17) has been considered and the corresponding right-hand side $\mathbf{w}$ has been obtained. A noise random vector $\boldsymbol{\eta}$, generated according to the description of section 8.1, has been added to $\mathbf{w}$. The relative norm 2 error is taken equal to 10^{-2}. The second experiment has the aim to find out how the noise affects the right-hand side of each system (29). Note that each right-hand side of (29) is obtained by rearranging the inverse FFT of the original vector $\mathbf{w} + \boldsymbol{\eta}$. It is well-known that the FFT, being an orthogonal transformation, does not alter the norm 2 of the absolute error. But it is important to investigate how each rearranged subvector is affected in terms of the relative error.

Since we make the hypothesis that the original image has small high frequency components and that the error affects only these components (if this hypothesis does not hold, no reconstruction is possible), the magnitude of the solutions of systems (29) tends to decrease when τ increases from 0 to $M/2$. It follows that the relative errors of the solutions of systems (29) increase when τ increases from 0 to $M/2$, and that only the systems (29) corresponding to low indices τ should be used for a significant reconstruction.

8.3 - Choice of the method. We examine the three regularizing methods for the solution of each system (29). The size of the system is $K \times K$, hence each iteration of the CG has a cost of K^2 operations. Also the cost of Tikhonov method (once the optimal parameter has been determined and the Choleski factorization has been performed) is of K^2 operations. The SVD (once the singular value decomposition has been performed) requires $2nK$ operations, where n is the number of singular values considered. Hence, if n does not depend on K, the cost of the SVD is linear with K. Due to the large number of systems (29) to be solved, these computational considerations suggest to use the SVD, as long as n is sufficiently small and the reconstruction effectiveness is comparable with the other two methods.

The three methods have been tested in order to determine the best one from the point of view of the reconstruction effectiveness. It turns out that no significant differences exist among the obtained results, hence the SVD has been chosen for the subsequent experiments.

8.4 - Details of the SVD implementation. More experiments have been conducted with the aim of determining how many systems (29) should be solved in order to obtain the best possible reconstruction and how many singular values should be used for the computation.

The tests show that the contribution to the solution becomes negligible when considering systems whose first singular value is lower than $0.05\sigma_1$, σ_1 being the largest singular value of the first block. This accounts for the half of systems (29). The solution of the discarded systems (29) is directly set equal to zero. The remaining systems are solved by the SVD using only a fixed number of singular values. The experiments have shown that two singular values are sufficient.

9 The algorithm

The algorithm is composed of two phases:

(a) a preprocessing phase, where the required matrices are constructed,

(b) a substitution phase where the vector $\mathbf{g}$ of the measured data is processed.

Of course only the second phase is required for any new data vector. In any case we assume that the noise level of the data is known.

9.1 - Preprocessing phase.

1 - Initialize the constants, compute the vectors of the nodes ϕ_m, $m = 0, \ldots, M-1$, and s_k, $k = 0, \ldots, K-1$.

2 - Compute the values a_i, $i = 0, \ldots, \omega$ and scale them. Let *scal* be the scaling factor. For $\omega = 12$ the already scaled values are in (31). Supply a routine $mult(A, \mathbf{x})$ for computing the multiplication of the symmetric Toeplitz matrix A with the given coefficients for any vector $\mathbf{x}$.

3 - For any $k = 0, \ldots, K/2$ and $k' = k, \ldots, K-k-1$ compute the entries of the vector $\mathbf{b}$ by (32) and (33). Compute $\mathbf{d} = DFT(\mathbf{b})\sqrt{M}$ and set $(D_\tau)_{kk'} = d_{kk'}$.

4 - For $\tau = 0, \ldots, M/2$ consider the matrices C_1 and C_2 defined in (28) and construct matrix E_τ defined in (30). Compute the singular value decomposition of E_τ and store it only if the first singular value is greater than σ_1, according to subsection 8.4.

9.2 - Substitution phase.

5 - For $p = 0, \ldots, P-1$, let $\mathbf{w}$ be the vector of entries $w_l = g_{lP+p}$, $l = 0, \ldots, L-1$. Apply CG method for 2 iterations. Let $\mathbf{u}$ be the solution thus computed. Insert $\mathbf{u}$ into the corresponding place of vector $\mathbf{y}$, that is $y_{lP+p} = u_l$, $l = 0, \ldots, L-1$. Multiply $\mathbf{u}$ by *scal*.

6 - For $l = 0, \ldots, L-1$ let $\mathbf{w}$ be the vector of entries $w_p = y_{lP+p}$, $p = 0, \ldots, P-1$. Construct vector $\mathbf{v}$ as follows: for any $k = 0, \ldots, K-1$, let $\mathbf{w}^{(k)}$ be the vector of entries $w_m^{(k)} = w_{mK+k}$, $m = 0, \ldots, M-1$. Compute $\mathbf{f}^{(k)} = IDFT(\mathbf{w}^{(k)})$ and let $v_{mK+k} = f_m^{(k)}$, $m = 0, \ldots, M-1$.

7 - Construct vector $\mathbf{t}$ as follows: for $\tau = 0, \ldots, K/2$, let $\mathbf{z}$ be the vector of entries $z_k = v_{\tau K+k}$, $k = 0, \ldots, K-1$. Construct the right-hand side of system (29). Solve system (29) by applying the SVD to E_τ, if the corresponding decomposition has been stored. Construct vector $\mathbf{u}$ solution of (24). For $k = 0, \ldots, K-1$, let $t_{\tau K+k} = u_k$ and if $\tau \neq 0$ and $\tau \neq M/2$ let $t_{(M-\tau)K+k} = u_k$.

8 - Compute vector $\mathbf{u}$ as follows: for any $k = 0, \ldots, K-1$, let $\mathbf{t}^{(k)}$ be the vector of entries $t_m^{(k)} = t_{mK+k}$, $m = 0, \ldots, M-1$. Compute $\mathbf{f}^{(k)} = DFT(\mathbf{t}^{(k)})$ and let $u_{mK+k} = f_m^{(k)}$, $m = 0, \ldots, M-1$.

10 - Compute vector $\mathbf{h}$ of entries $h_{lP+p} = u_p$, $l = 0, \ldots, L-1$.

References

[1]M. Bertero, P. Boccacci, Introduction to Inverse Problems in Imaging, Institute of Physics Publishing, 1998.

[2] P. Boccacci, P. Bonetto, P. Brianzi, P. Calvini, F. Di Benedetto, A. R. Formiconi, A. Passeri, *The 2D+1 method for an Efficient Modelling of Collimator Blur in 3D SPECT imaging*, Ann. Univ. Ferrara, Sez. VII - Sc. Mat. Suppl. Vol. XIV (2000).

[3] P. Brianzi, F. Di Benedetto, *Exploiting Matrix Structures in SPECT models*, to appear in "Structured Matrices: Recent Developments in Theory and Computation", D. Bini, E. Tyrtyshnikov and P. Yalamov eds., Nova Science Publisher Inc., New York, 2000.